Reconstruction of Si(001) and adsorption of Si adatoms and ad-dimers on the surface: Many-body potential calculations

Jun Cai[1,2] and Jian-Sheng Wang[1]
[1]*Singapore-MIT Alliance and Department of Computational Science, the National University of Singapore, Singapore 119260, Republic of Singapore*
[2]*Department of Physics, Beijing Normal University, Beijing 100875, P. R. China*
(Received 25 August 2000; revised manuscript received 20 December 2000; published 14 June 2001)

A recently developed potential function for covalent materials [Phys. Status Solidi B **212**, 9 (1999)] is used to simulate the reconstruction of the Si(001) surface, the surface adsorption, and diffusion of Si on the surface. For the simulation of reconstruction of Si(001) surface, our numerical results show that an empirical potential can correctly predict buckling-dimerized asymmetrical (001)-(2×1), p-(2×2), and c-(4×2) configurations and the relative stability between them in energetics. For the calculations of surface adsorption, we consider the formation energies and diffusion activation energies of several possible binding sites. The predicted stable and metastable configurations and diffusion paths of Si adatom and Si ad-dimers on the Si(001)-(2×1) surface are in agreement with those from first-principles calculations and experiments.

DOI: 10.1103/PhysRevB.64.035402 PACS number(s): 68.35.Bs, 71.15.−m, 68.03.Fg

I. INTRODUCTION

For the understanding of the microscopic structure and microscopic dynamic process of atoms in materials science, an essential ingredient is to obtain a reliable and accurate interactive potential function. Although there have existed many excellent works in this aspect,[1–8] it still cannot satisfy our eager wishes for a complete description of a complex microscopic system, such as those characterized by a large number of degrees of freedom, lack of symmetry, etc. This is due to the fact that on the one hand, ideally, using the first-principles technique one may investigate various complex microscopic phenomena involving materials science, but an unbearable computer cost makes this desire unfulfilled. On the other hand one may draw support from an empirical or semiempirical method in these researches, but this will sacrifice computational accuracy. Until now, we still linger on this situation for an investigation of microscopic process. But, fortunately, for a large-scale system this kind of empirical or semiempirical method may be feasible, as long as we do not fuss about computational precision too much quantitatively. In the following, we may see several such examples.

We have developed an empirical method for covalent materials recently.[9] This method is based on electronic density-functional theory. It only includes five potential parameters and has an analytical functional form. This function has been used to study bulk defects, symmetrical reconstruction of the (001) surface, small clusters, concerted exchange path, bulk phase stability, and shear properties of Si.[9] In this paper, the potential function is used further to study the reconstruction of the Si(001) surface as well as the adsorption and diffusion properties of Si adatom and Si dimer on the surface. For the simulation of reconstruction of the Si(001) surface, our numerical results show that the surface prefers a buckling-dimerized asymmetrical (001)-(2×1) configuration to a dimerized symmetrical (001)-(2×1) structure in energetics. In this simulation a p-(2×2) reconstruction and a c-(4×2) reconstruction are also predicted and their energies are lower than the energies of the (2×1) configurations. These properties predicted are consistent with the first-principles calculations, qualitatively. We have shown that an empirical potential can predict correctly buckling-dimerized asymmetrical (2×1), p-(2×2), and c-(4×2) reconstructions of Si(001) surface and the relative stability between them. For the calculations of surface adsorption, we consider the formation energies and diffusion-activation energies of several possible binding sites. The predicted stable and metastable configurations and diffusion paths of Si adatom and Si ad-dimer on the Si(001)-(2×1) surface are in agreement with those from first-principles calculations and experiments. In addition, a quantitative energetics of surface reconstruction and adsorption of small Si on the Si(001)-(2×1) surface have been determined using both first-principles methods and empirical-potential methods. We also did a detailed comparison between these results and ours. It is found that these models have their respective merits, and they are mutually complementary for the description of microscopic systems.

II. THEORY AND METHOD

Our model is inspired by the embedded-atom method.[8,10] In the theoretical framework of an embedded-atom method the total energy of a system can be written as

$$E_{tot}=\sum_i F_i(\rho_i)+\frac{1}{2}\sum_{i\neq j}\phi(r_{ij}). \tag{1}$$

In the above equation, $\phi(r_{ij})$ is the pair interaction related to a specified pair of atoms i and j separated by a distance r_{ij}, $F_i(\rho_i)$ is called the embedded-atom energy, and ρ_i denotes the local electron density at atom i and is assumed to be a linear superposition of individual atomic-electron densities. In general, the linear-superposition approximation works well for close-packed systems due to very high symmetry in structure, but it does not work for covalent materials, where a lower symmetry is present. In this case, we have

shown that due to the screening effect of electron density, the local electron density may be rewritten as[9]

$$\rho_i = \sum_{j(\neq i)} s_{ij} f(r_{ij}). \tag{2}$$

In the above formula $f(r)$ denotes individual atomic-electron density, and the linear superposition approximation of $f(r)$ has been replaced by a nonlinear superposition of $f(r)$. The coefficient s_{ij} expresses the screening effect of electron density and it has the following simple form:

$$s_{ij} = \prod_{k(\neq i,j)} s_{ijk} = \prod_{k(\neq i,j)} \exp(-g_{ijk}) = \exp\left(- \sum_{k(\neq i,j)} g_{ijk} \right) \tag{3}$$

with

$$g_{ijk} = \begin{cases} 0 & \text{if } r_{ik} + r_{jk} - r_{ij} \geqslant 2r_{ij} \\ \dfrac{r_{ij}}{r_e}\left(\dfrac{r_{ij}}{r_{ik} + r_{jk} - r_{ij}} - \dfrac{1}{2} \right)^n & \text{for the rest} \\ \infty & \text{if } r_{ik} + r_{jk} - r_{ij} = 0. \end{cases} \tag{3a}$$

The physical and geometrical meanings of the screen coefficient s_{ijk} have been illustrated in Ref. 9 in detail. We do not repeat it again here. The $f(r)$, $F(\rho)$, and $\phi(r)$ have the following analytic forms:[9]

$$f(r) = f_e \exp[-\alpha(r - r_e)], \tag{4a}$$

$$F(\rho) = \left[\ln\left(\frac{\rho}{\rho_e} \right)^\gamma - 1 \right] \left(\frac{\rho}{\rho_e} \right)^\gamma F_0 + \left(\frac{\rho}{\rho_e} \right) F_1, \tag{4b}$$

and

$$\phi(r) = \phi_0 \exp[-\beta(r/r_e - 1)]. \tag{4c}$$

In the above formulas r_e and ρ_e are the nearest-neighbor distance and the local electron density, respectively, at the equilibrium diamond structure; n and γ are two constants. In general, n is fixed to be 3 and γ is taken as 1.80. The f_e is a scaling factor and is taken as 1 for a pure system. The rest of the parameters are $\alpha = 1.515\,657$ Å^{-1}, $\beta = 4.928\,263\,8$ Å^{-1}, $\phi_0 = 3.572\,977$ eV, $F_0 = 0.276\,114\,2$ eV, and $F_1 = -12.712\,026$ eV. The cutoff distance r_{cut} is set to $1.2a_0$, a_0 is the lattice constant. All these parameters and constants are obtained directly from Ref. 9. At the present we apply the potential function to study the reconstruction of the Si(001) surface and the adsorption of Si on it. The minimization of energy is searched by a conjugate-gradient method.

In our calculations, the computational cell is a 21-layer-thick slab with 64 atoms in each layer. The cell includes 1344 atoms. Periodic boundary conditions are applied in an XY plane of the cell. The XY plane contains X and Y axes. The X axis is along [110] direction and the Y axis is along $[1\bar{1}0]$ direction, thus, the XY plane contains the (001) surface of the lattices. The atoms of the bottom-most nine layers (in the direction of Z) of the lattice are held rigid. The other atoms are allowed to relax fully so as to obtain a configuration with minimal energy for this system.

TABLE I. Atom displacements of the first six atomic layers relative to their bulk-terminated positions, the total energy E_{tot}, and the bond length b_l for the (2×1) reconstruction. The atom labeling scheme is explained in Fig. 1. In the table asymmetric-buckling-dimerized (2×1) reconstruction is noted using $(2\times1)a$, where ''a'' stand for asymmetric.

Atom	(2×1) δy (Å)	δz (Å)	$(2\times1)a$ δy (Å)	δz (Å)
11	0.7640	−0.1314	0.6942	−0.0703
12	−0.7640	−0.1314	−0.7685	−0.0418
21	0.1099	0.0916	0.0669	0.1335
22	−0.1099	0.0916	−0.1628	0.1657
31	0.0000	0.1492	−0.0401	0.2388
32	0.0000	−0.0801	−0.0238	−0.0443
41	0.0000	0.0565	−0.0182	0.1136
42	0.0000	−0.0484	−0.0080	−0.0178
51	−0.0104	0.0011	−0.0209	0.0264
52	0.0104	0.0011	0.0113	0.0214
61	−0.0040	0.0003	−0.0065	0.0079
62	0.0040	0.0003	0.0052	0.0061
b_l (Å)	2.2904		2.3569	
E_{tot} (eV)	−3194.826		−3196.201	

III. RESULTS AND DISCUSSION

A. Si(100) surface reconstruction

As did by Petukhov *et al.*, for C,[11] we perform simulations for the above computational cell for Si. Upon relaxation of the system the free surface dimerizes. According to different initial configurations two kind of stable reconstructed (2×1) surfaces, one kind of p-(2×2) reconstruction, and one kind of c-(4×2) configuration can be obtained. The atom displacements, the bond lengths b_l of dimers, and the total energies E_{tot} of relaxed atoms in these reconstructed systems are listed in Tables I and II.

From Table I, we can see that for the (2×1) reconstruction, one of them is a symmetric-dimerized surface, the other is an asymmetric-dimerized surface (the dimerized rows are formed due to the movement of atom rows of the topmost layer relative to each other in the Y direction). In the symmetric reconstruction the dimers are not buckled while in the asymmetric one the dimers are buckled due to the asymmetrical relaxation of atom rows in the topmost layer in the Z direction. In fact, in the present calculations, for the so-called symmetrical (2×1)-surface system an asymmetrical relaxation occurs in the Z direction in its deeper layers while in the Y direction the relaxations are symmetrical. For the asymmetrical (2×1)-surface system, not only in the Z direction but also in the Y direction, an asymmetrical relaxation occurs in its topmost layer and its deeper layers. For Si(001) (2×1) we also find that the energy of the symmetric-(2×1) surface is 0.043 eV per dimer over one of the

TABLE II. Same as Table I, but for p-(2×2) and c-(4×2) reconstructions of the Si(001) surface. The data in the brackets denote the deviations of atom sites adjacent to the unit cell as shown in Fig. 1 from the ideal Si(001) surface.

	p-(2×2)			c-(4×2)		
Atom	δx (Å)	δy (Å)	δz (Å)	δx (Å)	δy (Å)	δz (Å)
11	0.0000	0.7654(0.7583)	−0.0699(−0.1581)	0.0000	0.7582(0.7654)	−0.1581(−0.0699)
12	0.0000	−0.7583(−0.7654)	−0.1581(−0.0699)	0.0000	−0.7654(−0.7582)	−0.0699(−0.1581)
21	−0.0068(0.0068)	0.1443	0.1377	0.0069(−0.0068)	0.1443	0.1377
22	0.0068(0.0068)	−0.1443	0.1377	−0.0068(0.0068)	−0.1443	0.1377
31	0.0000	0.0000	0.3093	0.0022(−0.0022)	0.0000	0.3093
32	0.0000	0.0000	−0.0844	0.0000(0.0000)	0.0000	−0.0844
41	0.0000	0.0003(−0.0003)	0.0989	0.0000	0.0000	0.0986(0.0993)
42	0.0000	−0.0007(0.0007)	−0.0179	0.0000	0.0007	−0.0179(−0.0179)
51	0.0000	−0.0058(−0.0057)	0.0100(0.0099)	0.0000	−0.0056(−0.0058)	0.0099(0.0100)
52	0.0000	0.0057(0.0058)	0.0099(0.0100)	0.0000	0.0058(0.0056)	0.0100(0.0099)
61	0.0000	−0.0023	0.0029	0.0000	−0.0023	0.0029
62	0.0000	0.0023	0.0029	0.0000	0.0023	0.0029
b_l (Å)		2.3177			2.3177	
E_{tot} (eV)		−3198.607			−3198.609	

asymmetric-(2×1) reconstructions. The bond lengths of the buckling dimers are 2.36 Å and this is slightly larger than the bond lengths of the nonbuckling dimers (2.29 Å). Note that in our previous calculations the bond length of the dimer was 2.439 Å, where we did not consider an asymmetric relaxation in the Y and Z directions.[9] In addition, the present potential predicts that the two atoms of a buckling dimer have a difference of 0.03 Å in their Z coordinates. The other empirical potentials gave the bond length of 2.20–2.352 Å, although in these works the effect of the buckling dimer could not be predicted.[12]

For the transition from the symmetrical-(2×1) reconstruction to the asymmetrical-(2×1) reconstruction, using the highly accurate *ab initio* pseudopotential calculations, the energy gain per dimer was the same as the value of 0.1 eV obtained in Ref. 13. Similar first-principles calculations by Kruger and Pollmann gave the results of 0.14 eV per dimer of the symmetric-dimerized surface over the buckling-dimerized asymmetric surface. The buckling amount, i.e., the difference in the height of the Si atoms of the asymmetric dimer was 0.73 Å and the dimer bond length was 2.25 Å.[14] The corresponding values of buckling amount and bond length presented by Kobayashi *et al.* were 0.54 Å and 2.26 Å, respectively.[15] The values by Yin and Cohen were 0.31 Å and 2.25 Å.[16] The recent *ab initio* calculation by Gay and Srivastava gave 0.62 Å and 2.25 Å.[17] Measured bond lengths were scattered in a wide range from 2.20 Å to 2.47 Å,[14] sensitively depending on the experimental method and on surface preparation. Thus, the results about the bond length of the dimer calculated from our present potential and the other empirical potentials are in agreement with those from the first-principles calculations and the experiments. Likewise, our model underestimates the energy gain and buckling amount of the buckling dimer as compared with the above first-principles calculations, but the trend is the same as these calculations. In fact, we also use the Tersoff potential[7] and the Stillinger-Weber (SW) potential[6] to do the same simulations. The Tersoff potential favors the symmetrical-(2×1) over the asymmetrical-(2×1) reconstruction in energetics. In the simulation, the buckling amount is calculated to be 0.05 Å and the asymmetrical reconstruction is 0.3 eV/dimer higher than the symmetrical one.[18] Using the Stillinger-Weber potential we cannot even find an asymmetrical-(2×1) reconstruction for the Si (001) surface.[19] Even so, the Tersoff potential and SW potential may be better than the present potential in some aspects, such as in the calculations of energy for fcc, bcc, and sc phases of Si.

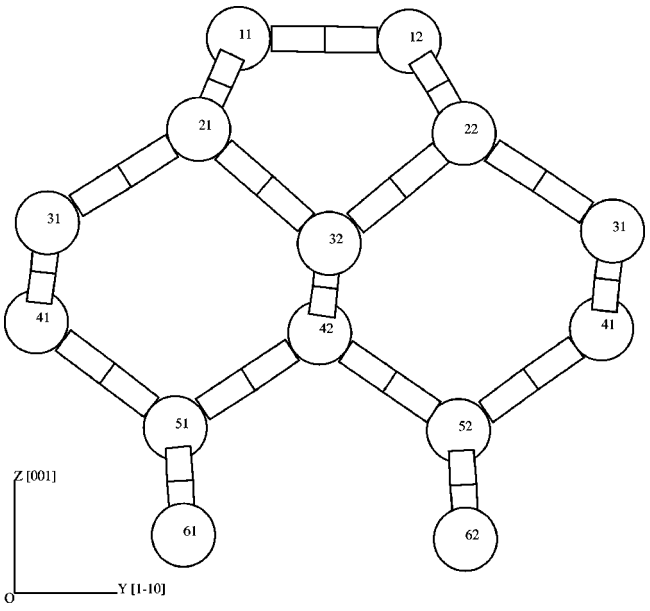

FIG. 1. The unit cell of Si(001)-(2×1) surface from the side (110) views.

Using the recently developed potential a p-(2×2) and a c-(4×2) reconstruction have been predicted. As shown in

Table II, the energies of the two configurations are found to be lower than the energies of the (2×1) configurations. The buckling amount and the bond length of the buckling dimer of the c-(4×2) reconstruction are predicted to be 0.088 Å and 2.3177 Å, respectively. For the p-(2×2) reconstruction, the buckling amount and the bond length are also calculated to be 0.088 Å and 2.3177 Å, respectively. From our numerical results we can also see that the atom displacements with respect to the ideal Si(001) surface are almost the same in the two structures. But the c-(4×2) structure is formed by alternating the tilt orientation of the buckling dimer along and across the dimer rows. In the p-(2×2) structure, the tilt orientation of the buckling dimer is alternated only along the dimer rows. In the two structures the atom displacement along the dimer rows in the second layer can be also observed. Moreover, the energy of the p-(2×2) structure is found to be almost the same as the energy of the c-(4×2) structure. These trends of the two structures are in agreement with the first-principles calculations, although the buckling amount in the present calculations is quite different from the one in the first-principles calculations. In first-principles calculations the buckling amount is predicted to be equal to 0.63 Å and 0.72 Å for p-(2×2) and c-(4×2) reconstructions, respectively,[20] and the p-(2×2) reconstruction is found to be 0.002 eV/dimer higher than the c-(4×2) reconstruction.[21] In addition, in the present numerical simulations, either for the (2×1) reconstruction or for the p-(2×2) and c-(4×2) reconstructions, we find that the relaxations contract the space between the first atomic layer and the second atomic layer and the second atomic layer lifts itself toward the surface. This somewhat conflicts with the first-principles calculations.[20,21] In the first-principles calculations, the space is predicted to be contracted while the second atomic layer is predicted to move toward the third atomic layer. Even so, we think that the present potential can describe the reconstruction of the Si(001) surface well.

As above, we also do the same calculations using smaller unit cells (16 atoms per layer). The results are completely identical to those using larger unit cells (64 atoms per layer).

It is worthy noting that, to our knowledge, in the previous calculations none of the empirical potentials can predict buckling-dimerized asymmetrical (2×1), p-(2×2), and c-(4×2) reconstructions of the Si(001) surface. A possible reason is that these potential models are all pure empirical models without an obvious quantum-mechanical background. Indeed, however, the expression for energy in the embedded-atom method can be derived from the local-density-functional theory.[22] On the bases of the embedded-atom method we consider an electron-screening effect and the screening function has an elliptical shape.[9] This physical origin is that when a covalent bond is formed by two atoms, say two hydrogen atoms, its electron cloud forms an ellipse roughly. From the above calculations we can see that the present potential model may work for the buckling phenomenon.

B. Si adatom on the Si(001)-(2×1) surface

We have shown that the present potential model may describe the Si(001)-surface reconstructions correctly. Going a step further we study the Si adatom on the surface.

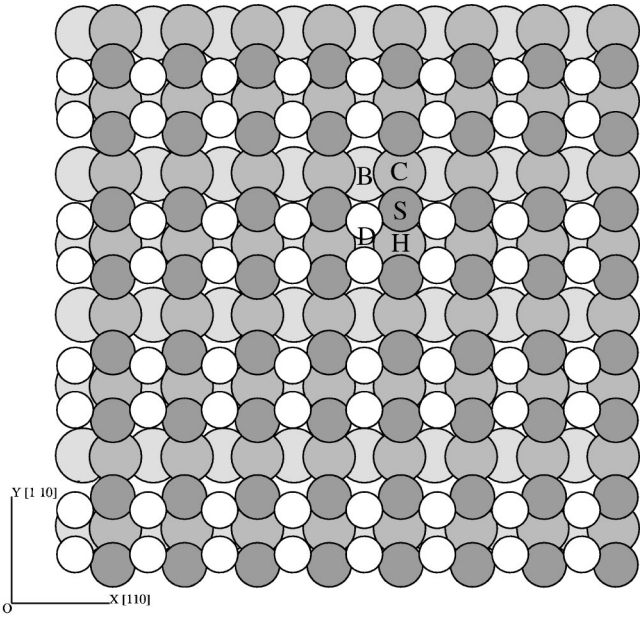

FIG. 2. Dimerized Si(001)-(2×1) surface denoting stable adatom sites by letters, where as a view guide, atomic radii increase gradually from top layer to bottom layer.

The energetics and geometry of the Si adatom on Si(001) (2×1) has been widely studied by the first-principles calculations and empirical methods.[24–28] These calculations predict that if an Si atom is added to the dimerized (001) surface, it may occupy some stable or metastable adsorption positions. The typical positions may be seen in Fig. 2. But, about the energetics of these configurations, the empirical methods often provide a result that does not agree with that from first-principles techniques. In the following we investigate the five equilibrium positions once again using the present method.

In the present work, an Si atom is placed on the dimerized surface and the cell is fully relaxed again. We calculate the binding energy, diffusion activation energy, and the height above the ideal Si(001) surface for adatoms at these positions. The results, together with those from experiments, the other empirical potentials, and first-principles calculations are listed in Table III. From the table we can see that the binding energies gradually decrease for site *S*, *D*, *H*, *C*, and *B* in order in our calculations, i.e., site *S* is predicted to be the lowest-energy site and site *D* is the second-lowest-energy position. The binding energies of site *C* and site *B* in the trough between dimer rows are found to be smaller than those of site *H*, site *D* at the top of dimer rows, and site *S* at the trough. Using the first-principles technique in local density approximation (LDA) Smith *et al.* found that this arrangement was in the order *S*, *H*, *D*, *B*, *C* while the calculation with the Perdew-Wang gradient correction gave the order of *S*, *D*, *H*, *B*, *C*. The later [with gradient correction (GC)] was believed to be more reliable than the former.[25] Thus, by first-principles calculations with GC, Smith *et al.* also found that the site *S* was the lowest-energy position and *D* was the second-lowest-energy site, the binding energies of positions *B* and *C* were smaller than those of site *H*, *D*, and

TABLE III. Adatom binding energies E_b (eV), diffusion activation energies E_a (eV), and the height z (Å) above the ideal (100) surface. $\|d$ and $\perp d$ are the processes of diffusion parallel and normal to a dimer row, respectively.

Site		Baskes[a]	Exp.[b]	This work	LDA[c]	GC[c]	SW	Tersoff[c]
	E_b	3.67		1.3	3.85	3.25	3.16[c]	3.51
B	z			0.623	−0.69		1.31[c]	1.22
	E_b	3.598		3.6	4.71	4.30	2.46[c]	3.08
S	z			0.94	0.72		1.92[c]	1.67
	E_b	3.04		1.7	3.63	2.92	1.23[c]	2.31
C	z			−0.114	−1.07		0.92[c]	0.61
	E_b	3.49		2.8	4.19	3.74	1.57[c]	2.68
H	z			1.255	1.33		1.88[c]	1.47
	E_b	3.29		3.2	4.09	3.81	2.70[c]	3.27
D	z			1.80	1.97		1.54[c]	1.63
E_a	$\|d$	0.74	0.67±0.08	1.6	0.4,0.6[d]	0.2	0.3[e]	0.7
E_a	$\perp d$	0.98	≈1	2.8	1.0,1.0[d]	1.5	0.7[e]	0.43

[a]Reference 24.
[b]Reference 29.
[c]Reference 25.
[d]Reference 28.
[e]Reference 27.

S. In addition, in the first-principles calculations of Tsuda *et al.*, either for the spin-triplet state or for the spin-singlet state, the binding energies of *H*, *D*, and *S* were all predicted to increase gradually in order.[26] These results are in good agreement with our calculations. Compared with these results, Zhang *et al.*[27] and Smith *et al.*[25] using the Stihlinger-Weber (SW) silicon potential,[6] predicted the lowest-energy position to be position *B* and the second-lowest-energy site to be site *D*. Similarly, using the Tersoff potential[7] Smith *et al.*[25] gave the conclusions identical to those of Zhang *et al.* using the SW potential. Using the modified embedded-atom method (MEAM) (Ref. 23) Baskes presented that site *S* was not the lowest-energy position, although the energy was very close to the lowest energy of site *B* in his calculations. Hence, the results from these three empirical potentials are conflicting with those from first-principles calculations and the present-model calculations for the prediction of the lowest-energy site. But, these empirical potentials, except the present potential model, all predict that site *C* has the smallest binding energy (the greatest-energy configuration) in these sites. This is in agreement with first-principles calculations.

In order to study a diffusion path, activation energies for transition states between trough and top positions as well as for migration from the trough to top locations are calculated. In these calculations the adatom position along the transition path is restricted to lie in a plane whose normal is along the line connecting the equilibrium points. The energy of the system for a number of planes along this line is calculated and the activation energy is taken as the highest energy, relative to lower minimum energy in the diffusion path. We consider four paths: the diffusion paths parallel to dimer rows *D*-*H*-*D* at the top and *B*-*C*-*B* at the trough, and the diffusions normal to dimer rows *H*-*S*-*C* and *D*-*B*-*D*. We find that the activation energy (not shown here) is the highest for *D*-*B*-*D* diffusion while the lowest activation energy corresponds to *B*-*C*-*B* (0.7 eV). The activation energies for paths *D*-*H*-*D* and *H*-*S*-*C* are 1.6 eV and 2.8 eV, respectively. From these results we may conclude that the migration of an atom at the trough along the dimer rows is significantly easier than that at the top along the dimer rows. But, note that the binding energies of site *C* and site *B* are far smaller than site *D*, site *H*, and site *S*. This leads to the fact that adatoms at site *C* and site *B* are far fewer than ones at positions *D*, *H*, and *S*. Thus the diffusion occurs far more scarcely along *B*-*C* than along *D*-*H*. Moreover, for the adatoms at the top of dimer rows, the activation energy (2.8 eV) of diffusion normal to dimer rows is far greater than the activation energy (1.6 eV) of diffusion parallel to dimer rows. Thus, the diffusion may be the easiest along dimer rows (i.e., along *D*-*H*). This conclusion is in agreement with that from first-principles calculations, although those activation energies are overestimated in our calculations. In first-principles calculations, Brocks *et al.*[28] considered the path of diffusion along the dimer rows and the path of diffusion perpendicular to the dimer rows, obtaining activation barrier heights of 0.6 V and 1.0 eV, respectively. Simth *et al.* gave an activation energy of 0.4 eV for the parallel path and one of 1.0 eV for the lowest-energy paths for perpendicular diffusion.[25] In the previous empirical potential calculations, using MEAM, Baskes[24] predicted that diffusion normal to the dimer row occurred with an activation energy of 0.98 eV and diffusion parallel to dimers rows occurred with the activation energy of 0.74 eV. Zhang *et al.*[27] using the SW potential found that migration along the dimer rows occurred with an activation energy of 0.3 eV and along the activation barrier, from top to trough, 0.7 eV. These are identical to first-principles calculations. But using the Tersoff potential Simth *et al.* gave the corresponding energies of 0.7 and 0.3 eV,[25] which is in conflict with first-principles calculations. Although, these results from the previous empirical potentials as well as first-principles calculations are more close to the experimental data[29] of the activation energies than those from the present method, the stable configurations and diffu-

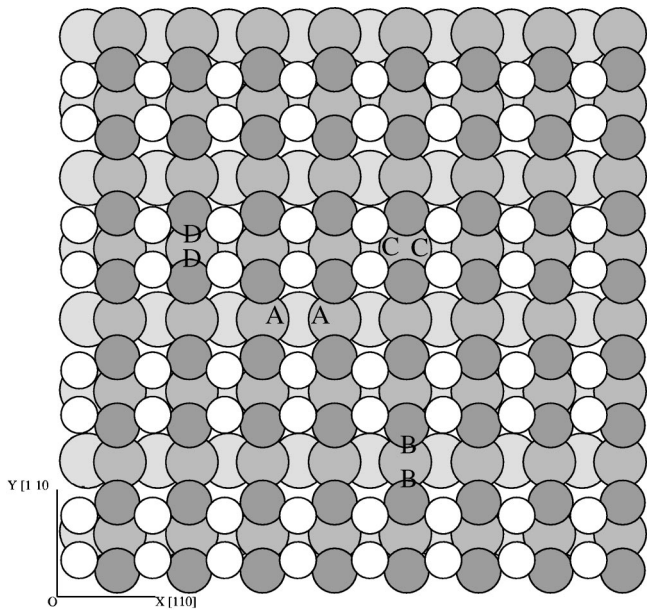

FIG. 3. Dimerized Si(001)-(2×1) surface denoting stable ad-dimers by letters, where as a view guide, atomic radii increase gradually from top layer to bottom layer.

sion paths predicted from the present potential are in agreement with those from first-principles calculations.

Finally, from Table III we may see that the heights of the adatom over ideal Si(001), except the *B*-adatom, calculated using the present potential model are very close to the results from first-principle calculations for adatoms at *S*, *C*, *H*, and *D* sites. For this prediction, however, the results from the Tersoff potential and SW potential are not as good as our results, as compared with the results of first-principles calculations.

C. Si ad-dimer on Si(001)-(2×1) surface

A number of calculations have predicted that the migrating adatoms would interact with each other and form dimers. The present potential is also applied to investigate the geometry and energetics of these ad-dimers. The calculational procedure is exactly the same as above. Several equilibrium positions for ad-dimers are shown in Fig. 3. Our results, together with the other numerical results, are reported in Table IV. From the table we can see that the lowest equilibrium position for these ad-dimers is configuration *C*-*C* at the top of dimer rows parallel to dimer rows. For ad-dimer on the top of dimer row, the configuration *D*-*D* is normal to dimers rows and has an energy of 0.7 eV higher than *C*-*C*. In contrast to the ad-dimers at the top, for ad-dimers on the trough between the dimer rows, the normal ad-dimer *B*-*B* is more stable than the parallel ad-dimer *A*-*A*. Our results show that these ad-dimers are strongly bound with respect to dissociation into two isolated adatoms and *C*-*C* is the most stable configuration in these ad-dimers. This is exactly in agreement with the predictions by first-principles calculations.[30,31] The first-principle calculations indicated that the parallel dimer in the top *C*-*C* was the lowest-energy configuration. It was also predicted that these ad-dimers were strongly bound with respect to dissociation into two isolated adatoms. The *C*-*C* was more stable than *D*-*D* in energy. For the ad-dimer at the trough the normal ad-dimer *B*-*B* was predicted more stable than the parallel ad-dimer *A*-*A*.[30,31] Baskes predicted the trough ad-dimer site *A*-*A* as the lowest energy configuration using MEAM.[24] This conflicts with first-principles results.

TABLE IV. Formation energies E_f (eV) with the reference to the lowest-energy configuration and diffusion-activation energies E_a (eV) of Si ad-dimers on the Si(001)-(2×1) surface. *r* denotes the rotation of the ad-dimer between the orientations of normal and normal to a dimer row. $\|d$ expresses the diffusion of the ad-dimer along a dimer row. *z* is the height over the ideal (001) surface.

Energy (eV)		Baskes[a]	Exp.	This work	Density function
$E_f^{A\text{-}A}$		0		3.4	0.76[b], 1.11[c]
$z^{A\text{-}A}$ (Å)				0.9925	
$E_f^{B\text{-}B}$		0.15		0.5	0.18[b], 0.31[c]
$z^{B\text{-}B}$ (Å)				0.8322	
$E_f^{C\text{-}C}$		0.68		0	0[b], 0.01[c]
$z^{C\text{-}C}$ (Å)				1.6298	
$E_f^{D\text{-}D}$		0.76		0.7	0.073−0.115[b]
$z^{D\text{-}D}$ (Å)				1.5598	
E_a	r	0.66	0.68±0.01[d]	3.3	1−1.2[d]
E_a	$\|d$	0.74	0.94±0.09[e]	4.2	1.45[b]

[a]Reference 24.
[b]Reference 30.
[c]Reference 31.
[d]Reference 32.
[e]Reference 33.

Our numerical results show that for the normal ad-dimer *B*-*B* or *D*-*D* the activation energy (not shown here) for a migration normal to dimer rows is far greater than the activation energy of 4.2 eV of *C*-*C* for the migration parallel to dimer rows. The activation energy for a rotation between the *C*-*C* state and *D*-*D* state is 3.3 eV. From these results it is easy to conclude that the parallel dimer can migrate by a process that includes rotation into the normal orientation, migration as a normal ad-dimer, and then rotation back to the parallel orientation. First-principle results predicted that the activation energy of the normal migration was larger than 1.45 eV of the parallel migration *C*-*C*, but the activation energy of *C*-*C* was greater than 1–1.2 eV for a rotation between the *C*-*C* configuration and the *D*-*D* configuration.[30,32] For the rotation and the parallel migration, the experimental data were (0.68 ± 0.01)[32] and (0.94 ± 0.09),[33] respectively. Using MEAM Baskes obtained the corresponding values to be 0.66 eV and 0.74 eV, respectively.[24] Compared with these results, our results overestimate the values but the anisotropic diffusions are predicted to be in agreement with first-principles calculations and experiments as well as the results of Baskes. Finally in Table IV we also give the height of the ad-dimer over the ideal Si(001) surface. It can be seen that dimer *C*-*C* and dimer *D*-*D* are higher over the ideal surface than dimer *A*-*A* and dimer *B*-*B*.

We should see that in the calculations above, although the atomic configurations are predicted to be in agreement with first-principles calculations, the magnitudes of the corresponding energies are usually poor as compared with first-principles calculations. One reason may be that the present potential gives too great a screening effect on electronic density when the system departs from an equilibrium state. This leads to the values of the calculated energies to be too high. In the previous calculations of bcc phase, fcc phase, and concerted exchange path for Si, the energies were overestimated.[9] The reason is the same as for the present calculations.

IV. SUMMARY

We have calculated the reconstruction and the adsorption of the Si(001) surface. The diffusion of the adatom and ad-dimer at the top of the dimer rows are predicted to be easier along the dimer rows than diffusion normal to the dimer rows. Also the stable configurations are found to be in agreement with those predicted by first-principles and experimental results. The present potential also predicts that a symmetrical-dimerizing Si(001)-(2×1)-surface reconstruction is 0.043 eV per dimer higher in energy than the asymmetrical buckling-dimerized Si(001)-(2×1) structure. The buckling amount and the bond length are 0.03 Å and 2.36 Å, respectively. At the same time the c-(4×2) and p-(2×2) reconstructions are also predicted and they are more stable than the (2×1) reconstruction. In the two structures the buckling amount and bond length of the dimer are found to be equal to 0.088 Å and 2.3177 Å, respectively. These results are all in agreement with first-principles calculations, at least, qualitatively. The present potential model may work for the description of the buckling phenomenon and adsorptions of adatom and ad-dimer on the Si(001) surface.

ACKNOWLEDGMENT

This work was supported by a Singapore-MIT Alliance Research Grant.

[1] W. Kohn and L. J. Sham, Phys. Rev. **140**, A1133 (1965); P. Hohenberg and W. Kohn, *ibid.* **136**, B 864 (1964).
[2] D. M. Ceperley and B. J. Alder, Phys. Rev. Lett. **45**, 566 (1980).
[3] U. von Barth and L. Hedin, J. Phys. C **5**, 1629 (1972).
[4] R. Car and M. Parrinello, Phys. Rev. Lett. **55**, 2471 (1985).
[5] C. Z. Wang, C. T. Chan, and K. M. Ho, Phys. Rev. Lett. **66**, 189 (1991).
[6] F. H. Stillinger and T. A. Weber, Phys. Rev. B **31**, 5262 (1985).
[7] J. Tersoff, Phys. Rev. B **38**, 9902 (1988).
[8] M. S. Daw and M. I. Baskes, Phys. Rev. B **29**, 6443 (1984).
[9] J. Cai, Phys. Status Solidi B **212**, 9 (1999).
[10] S. M. Foiles, M. I. Baskes, and M. S. Daw, Phys. Rev. B **33**, 7983 (1986); R. A. Johnson, *ibid.* **41**, 9717 (1990); A. Voter and S. P. Chen, in *Characterization of Defects in Materials*, edited by R. W. Siegel, J. R. Weertman, and R. Sinclair, Mater. Res. Soc. Symp. Proc. No. **82** (Materials Research Society, Pittsburgh, 1987), p. 175; M. W. Finnis and J. E. Sinclair, Philos. Mag. A **50**, 45 (1984); J. Cai and Y. Y. Ye, Phys. Rev. B **54**, 8398 (1996); J. Cai, Phys. Status Solidi B **203**, 345 (1997).
[11] A. V. Petukhov, A. Fasolino, D. Passerone, and F. Erolessi, Phys. Status Solidi A **174**, 19 (1999).
[12] H. Balamane, T. Halicioglu, and W. A. Tiller, Phys. Rev. B **46**, 2250 (1992).
[13] J. Dabrowski and M. Scheffler, Appl. Surf. Sci. **56**, 15 (1992).
[14] P. Kruger and J. Pollmann, Phys. Rev. Lett. **74**, 1155 (1995); Appl. Phys. A: Solids Surf. **59**, 487 (1994).
[15] K. Kobayashi, Y. Morikawa, K. Terakura, and S. Blugel, Phys. Rev. B **45**, 3469 (1992).
[16] M. T. Yin and M. L. Cohen, Phys. Rev. B **24**, 2303 (1981).
[17] S. C. A. Gay and G. P. Srivastava, Phys. Rev. B **60**, 1488 (1999).
[18] J. Cai and J.-S. Wang, Phys. Status Solidi B **223**, 773 (2001).
[19] J. Cai and J.-S. Wang (unpublished).
[20] R. Gunnela, E. L. Bullock, L. Patthey, C. R. Natoli, T. Abukawa, S. Kono, and L. S. O. Johansson, Phys. Rev. B **57**, 14 739 (1998).
[21] A. Ramstad, G. Brocks, and P. J. Kelly, Phys. Rev. B **51**, 14 504 (1995).
[22] M. S. Daw, Phys. Rev. B **39**, 7441 (1989).
[23] M. I. Baskes, Phys. Rev. B **46**, 2727 (1992).
[24] M. I. Baskes, Modell. Simul. Mater. Sci. Eng. **5**, 149 (1997).
[25] A. P. Smith, J. K. Wiggs, H. Jonsson, H. Yan, L. R. Corrales, P. Nachtigall, and K. D. Jordan, J. Chem. Phys. **102**, 1044 (1995).
[26] M. Tsuda, M. Hata, E.-I. Araki, and S. Oikawa, Appl. Surf. Sci. **107**, 18 (1996).
[27] Z. Y. Zhang, Y. T. Lu, and H. Metiu, Surf. Sci. Lett. **248**, L250 (1991).
[28] G. Brocks, P. J. Kelly, and R. Car, Phys. Rev. Lett. **66**, 1729 (1991).
[29] Y. W. Mo, J. Kleiner, M. B. Webb, and M. G. Lagally, Phys. Rev. Lett. **66**, 1998 (1991).
[30] T. Yamasaki, T. Uda, and K. Terakura, Phys. Rev. Lett. **76**, 2949 (1996).
[31] G. Brocks and P. J. Kelly, Phys. Rev. Lett. **76**, 2362 (1996).
[32] B. S. Swartzentruber, A. P. Smith, and H. Jonsson, Phys. Rev. Lett. **77**, 2518 (1996).
[33] B. S. Swartzentruber, Phys. Rev. Lett. **76**, 459 (1996).